

Recent results on dark sector searches at Belle II

Foteini Faidra Trantou^{a,b,*} on behalf of the Belle II collaboration

^a*Department of Physics, University of Pisa,
Via Filippo Buonarroti 3, Pisa, Italy*

^b*Istituto Nazionale di Fisica Nucleare,
Via Filippo Buonarroti 3, Pisa, Italy*

E-mail: foteini.trantou@phd.unipi.it

The Belle II experiment provides a unique opportunity to explore the dark sector, offering exceptional sensitivity to a broad class of models that propose light dark matter and dark mediators with masses between a few MeV/c^2 and GeV/c^2 . This paper reports the latest world-leading physics results from Belle II searches for an X resonance decaying into two muons, interpretable both as a Z' boson and a muonphilic dark scalar particle; long-lived (pseudo)scalars produced in B meson decays; inelastic dark matter in association with a dark Higgs boson as well as future prospects for other dark sector searches.

*Third Italian Workshop on the Physics at High Intensity (WIFAI2024)
12-15 November 2024
Bologna, Italy*

*Speaker

1. Introduction

Dark matter and dark sectors are among the leading motivations driving searches for physics beyond the Standard Model (SM). The dark sector postulates the existence of new, yet-undetected quantum fields, which mediate a feeble interaction between dark and visible matter. The existence of the dark sector and of a new fundamental interaction could provide a framework to address key unresolved questions in physics, such as the baryon-antibaryon asymmetry in nature or the anomalous magnetic moment of the muon $(g - 2)_\mu$, whose explanation is otherwise challenging due to the lack of non-SM phenomena at the electroweak scale [1]. These new interactions between dark matter and ordinary matter might occur via different "portals" and depend on the characteristics of the dark sector mediators, such as the mediator's spin and parity [2]. The main dark sector portals include the vector portal, mediated by dark photons; the scalar portal, which involves a mediator such as the Higgs boson or a new scalar particle; the neutrino portal, which utilizes fermionic mediators like heavy sterile neutrinos; and the pseudo-scalar portal, which involves axions or axion-like particles. High-precision experiments at the intensity frontier, such as the Belle II experiment, can probe the dark sector and detect new physics signatures. This paper gives an overview of the dark sector searches performed at the Belle II experiment with a dataset collected during the first data taking period 2019-2022.

2. The Belle II experiment

The Belle II experiment operates at the SuperKEKB e^+e^- asymmetric energy collider, an advanced facility located at KEK, Japan [3]. This experiment is a second-generation B factory, a major upgrade from the original Belle experiment, and is part of a broader effort to explore fundamental aspects of particle physics. Belle II is primarily optimized for the detection of B meson pairs, as well as D mesons and τ leptons, with particle collisions occurring predominantly at a center-of-mass energy of $\sqrt{s} = 10.58$ GeV, which corresponds to the $Y(4S)$ resonance. To date, the total integrated luminosity collected during Run I (2019–2022) and Run II (2024) has reached 575 fb^{-1} [4]. These runs were separated by a long shutdown period (LS1), during which the accelerator and the detector underwent significant maintenance and upgrades. The long-term objective is to accumulate 50 ab^{-1} , a dataset 50 times larger than that achieved by the Belle experiment.

2.1 Dark sector searches at Belle II

Although Belle II's primary focus is to study the properties of B mesons and their rare decays, the experiment also holds significant potential for dark matter (DM) discoveries. Belle II is highly sensitive to the presence of light dark sector mediators with a mass in the range between MeV/c^2 - GeV/c^2 . The unique advantages of B factories, such as detector hermeticity, well-defined initial conditions, and a clean experimental environment, enable excellent particle identification and high-precision measurements. These capabilities are crucial for reconstructing events with non-detectable particles and searching for invisible signatures, which are essential in detecting dark matter and exploring the dark sector. Additionally, dedicated triggers, such as single photon, single track, and single muon triggers, are implemented to study low-multiplicity and missing energy final states.

3. Recent results

Dark sector signatures can be investigated by searching for dark sector particles directly produced in e^+e^- collisions or emerging from the decay of mesons (such as B, D) and fermions (such as τ). Depending on the dark sector mediator and DM candidate mass hypothesis, different scenarios, with either visible, invisible or long-lived particle decays, arise. Belle II investigates these signatures to search for dark matter candidates such as the dark photon, axion-like particles or Z' bosons. It can also explore rare and exotic decay processes of known particles into dark sector states, aiming to uncover new physics beyond the SM. The most recent results on the experiment's dark sector searches are briefly presented below.

3.1 Search for a $\mu^+\mu^-$ resonance in four-muon final states

The $L_\mu - L_\tau$ model serves as the benchmark for this search, extending the SM by introducing a new vector gauge boson Z' [5]. This particle couples only to second and third generation SM leptons, with a coupling constant g' , but may also mediate interactions between SM and dark matter. Such new leptonic interactions could provide insights into the origin of the $(g-2)_\mu$ anomaly as well as the DM phenomenology and abundance. According to the model, the Z' could decay visibly to a pair of muons or taus, or invisibly to SM neutrinos or dark matter candidates.

We search for a $\mu^+\mu^-$ resonance in four-muon events via the process $e^+e^- \rightarrow \mu^+\mu^- X (\rightarrow \mu^+\mu^-)$, where X is radiated from one of the muons. The analysis probes two different models for the X resonance: it could be a Z' particle decaying visibly into a pair of muons or a muonphilic scalar S , which is a spin-0 boson that couples exclusively to muons through a Yukawa-like interaction [6]. The signature is a narrow peak in the invariant mass distribution of pairs of oppositely charged muons. Event selection focuses on four-track events, where at least three are identified as muons, with zero net charge and no extra energy. The main background contribution is $e^+e^- \rightarrow \mu^+\mu^-\mu^+\mu^-$ events and is suppressed using five neural networks trained in different X -mass ranges. This is achieved by exploiting distinctive kinematic features, such as the momentum distribution of muon tracks, to distinguish the signal from the background. For momenta above $0.7 \text{ GeV}/c^2$, muons are identified by their penetration into the outer KLM detector; at lower momenta, drift chamber and calorimeter data are used. The method retains 93%–99% of muons while rejecting 80%–97% of pions, depending on momentum.

The signal is extracted via maximum likelihood fits to the dimuon mass spectrum from $0.212 \text{ GeV}/c^2$ to $9.0 \text{ GeV}/c^2$, scanned in steps of the mass resolution with fit windows 60 times wider. The signal shape is modeled using two Crystal Ball functions with a shared mean, while the background is described by a quadratic function below $1 \text{ GeV}/c^2$ and a straight line above. We observe no significant excess using 178 fb^{-1} of data and set 90% confidence level (CL) upper limits on the cross section $\sigma(e^+e^- \rightarrow \mu^+\mu^- X) \times \mathcal{B}(X \rightarrow \mu^+\mu^-)$, ranging from 0.046 fb to 0.97 fb for the $L_\mu - L_\tau$ model and from 0.055 fb to 1.3 fb for the muonphilic scalar model [7]. Results are presented in Figure 1. These limits are subsequently translated in terms of upper limits on the coupling constants of these processes. For masses below $6 \text{ GeV}/c^2$, they range from 0.0008 to 0.039 for the $L_\mu - L_\tau$ model and from 0.0018 to 0.040 for the muonphilic scalar model. As illustrated in Figure 2 (left), the obtained results are competitive with existing constraints on the g' coupling, despite using a significantly smaller integrated luminosity sample (178 fb^{-1} , compared to 514 fb^{-1}

at BaBar and 643 fb^{-1} at Belle). Additionally, in Figure 2 (right), we set the first limits for the muonphilic scalar model from a dedicated search.

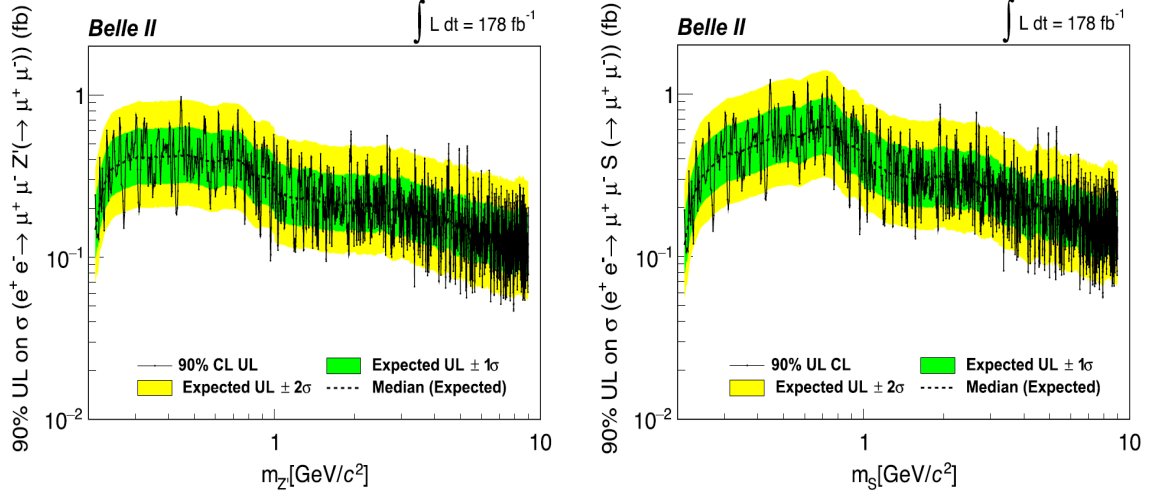


Figure 1: Observed 90% CL upper limits and corresponding expected limits on the cross sections for the processes $e^+e^- \rightarrow \mu^+\mu^-X (\rightarrow \mu^+\mu^-)$, where $X = Z'$ or S , as a function of $m_{Z'}$ (left) and as a function of m_S (right).

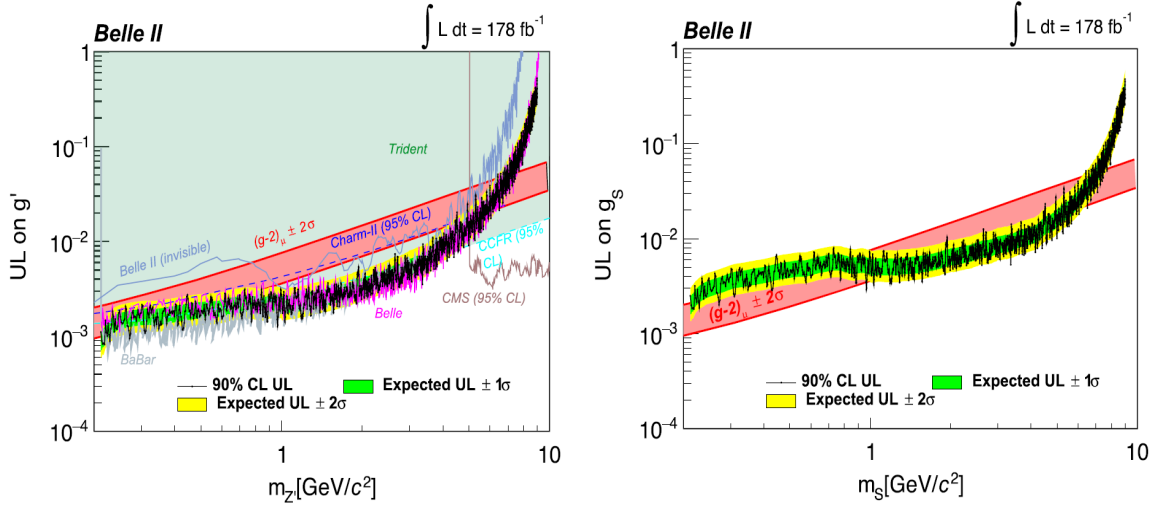


Figure 2: Observed 90% CL upper limits and corresponding expected limits on the $L_\mu - L_\tau$ model coupling constant g' as a function of $m_{Z'}$ (left) and the muonphilic scalar model coupling constant g_S as a function of m_S (right).

3.2 Search for a long-lived (pseudo)scalar in $b \rightarrow s$ transitions

This search is based on a promising extension of the SM that introduces a new spin-0 light scalar S mediator that could be produced in $b \rightarrow s$ quark transitions [8]. The particle may give mass to DM particles and interact with the SM Higgs boson through a mixing angle θ . For small values of that mixing angle, S can be a naturally long lived particle. If the mass of the S particle is below the mass of the B meson, then decays of S into DM particles must be kinematically forbidden

to provide the correct relic density. Therefore, this search is motivated to look for S decays into SM particles.

The analysis strategy relies on searching for an excess in the invariant mass distribution of opposite-charged tracks originating from a displaced vertex, accompanied by a charged kaon. In particular, we investigate S decays into SM particles in eight different channels within $\mathcal{B}^0 \rightarrow K^{*0}(\rightarrow K^+\pi^-)S$ and $\mathcal{B}^+ \rightarrow K^+S$ events, where $S \rightarrow x^+x^-$ ($x = e, \mu, \pi, K$). The main background sources are the combinatorial $e^+e^- \rightarrow q\bar{q}$ events, suppressed by requiring consistent kinematics with the B-meson decay, and the long lived K_S^0 particle, whose mass region is excluded from the search and used as control sample in data to evaluate systematic uncertainties. For the signal extraction, we perform extended maximum likelihood fits to the reduced invariant mass $m_S = \sqrt{M_{S \rightarrow x^+x^-}^2 - 4m_x^2}$. This selection improves notably the modeling of the signal width close to the kinematic thresholds, where momentum and angle uncertainties dominate the resolution. Using the reduced mass mitigates these effects with the well-known rest mass contribution, yielding more stable resolution near threshold.

We do not observe any significant excess using a sample of $N_{B\bar{B}} = (198 \pm 3) \times 10^6$ B-meson pairs, corresponding to an integrated luminosity of 189 fb^{-1} [9]. We set model-independent upper limits at 95% C.L. on the product of branching fractions $\mathcal{B}(B \rightarrow KS) \times \mathcal{B}(S \rightarrow x^+x^-)$ as a function of the scalar mass m_S for various S lifetime hypotheses in the range $0.001 < c\tau < 100 \text{ cm}$. The obtained results are shown in Figure 3, where we set the first limits on S for exclusive hadronic and for e^+e^- final states. We subsequently translate the results to constrain the $(\sin\theta - m_S)$ parameter space, defined by the sine of the mixing angle θ and the S invariant mass. In addition, the results are reinterpreted in an axion-like particle (ALP) benchmark model with f_α coupling to fermions [10]. Results both for the dark scalar S and the ALP scenario are shown in Figure 4.

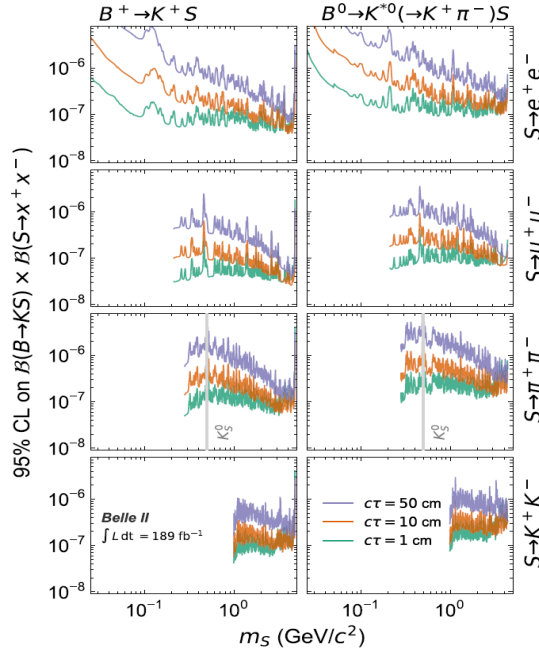


Figure 3: Observed 95% CL upper limits on $\mathcal{B}(B \rightarrow KS) \times \mathcal{B}(S \rightarrow x^+x^-)$ as a function of m_S for different S lifetimes $c\tau$. The mass region corresponding to the fully-vetoed K_S^0 for $S \rightarrow \pi^+\pi^-$ is marked in gray.

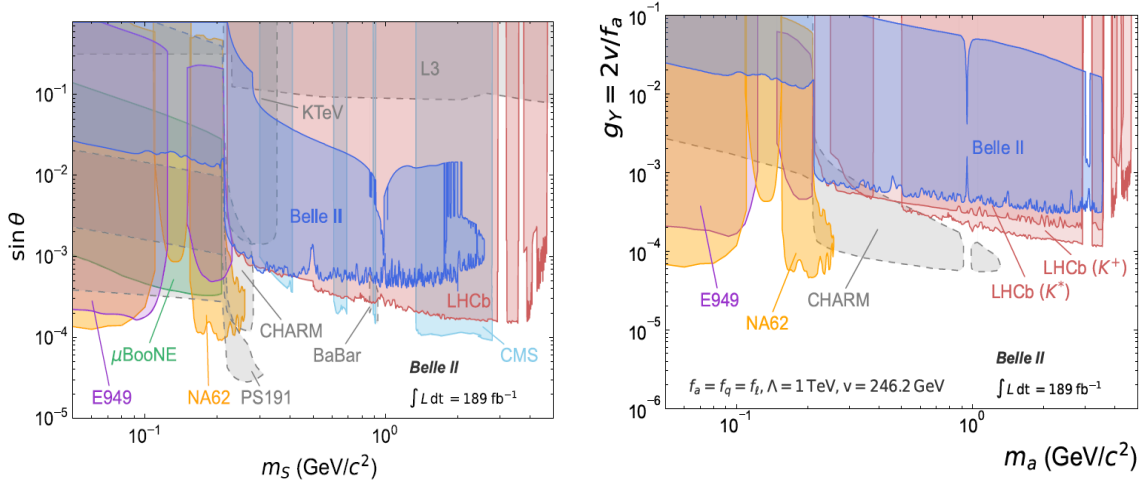


Figure 4: Exclusion regions at 95% CL in the $(\sin\theta - m_S)$ plane (left) and $(g_\gamma - m_a)$ plane (right), where $g_\gamma = 2v/f_a$ is the ALP coupling constant with the vacuum expectation value v , from this work (blue) together with existing constraints from various experiments.

3.3 Search for inelastic dark matter and a dark Higgs boson

A non-minimal class of dark sector models introduces inelastic DM (iDM), where DM couples inelastically to SM states [11]. The simplest among them can reproduce the observed relic dark matter density without violating cosmological limits, featuring two dark matter particles, χ_1 and χ_2 , and a massive dark photon A' [12]. The A' interacts with the SM photon via a kinetic mixing mechanism at strength ϵ and with DM via the coupling $g_D = \sqrt{4\pi\alpha_D}$, while it decays predominantly via $A' \rightarrow \chi_1\chi_2$. A small mass splitting Δm between the two dark matter particles χ_1 and χ_2 , with $m_{\chi_2} > m_{\chi_1}$, is induced by a dark Higgs field and a corresponding dark Higgs boson h' . This mass gap makes the heavier state χ_2 long-lived before decaying into a pair of SM particles and the lighter state χ_1 , while χ_1 is stable (relic candidate) and escapes the detector. The h' may interact with the SM Higgs via a mixing angle θ , rendering it naturally long-lived for small values of θ , and couples to DM via the coupling $k \approx g_D \Delta m / m_{A'}$.

We search for a dark Higgs h' produced in association with iDM through the process $e^+e^- \rightarrow h'(\rightarrow x^+x^-)A'(\rightarrow \chi_1\chi_2(\rightarrow \chi_1e^+e^-))$ where $x^\pm = \mu^\pm, \pi^\pm, K^\pm$ and $m_{h'} < m_{\chi_1} < m_{A'}$. The analysis aims to identify an excess in the h' invariant mass distribution in four-track events featuring up to two displaced vertices and missing energy. The signal signature consists of two tracks forming a displaced vertex that points back to the interaction point (IP) and two tracks forming a non-pointing displaced vertex, corresponding to h' and χ_2 in signal events respectively. Background levels are expected to be close to zero as the selection criteria exploit the signal signature to minimize them: we require at least one vertex displaced sufficiently from the IP in order to suppress prompt SM contributions, the h' vertex pointing back to the IP, a track opening angle > 0.1 rad to suppress photon conversions, and missing energy > 4 GeV to reject remaining SM backgrounds. Other background sources include the long lived K_S^0 and Λ particles as well as the ϕ resonance, whose mass regions are excluded from the search and studied as control data samples.

In the absence of an additional signal, fewer than 10 events are expected in the combined final states of the dark Higgs, based on SM background simulations corresponding to an integrated

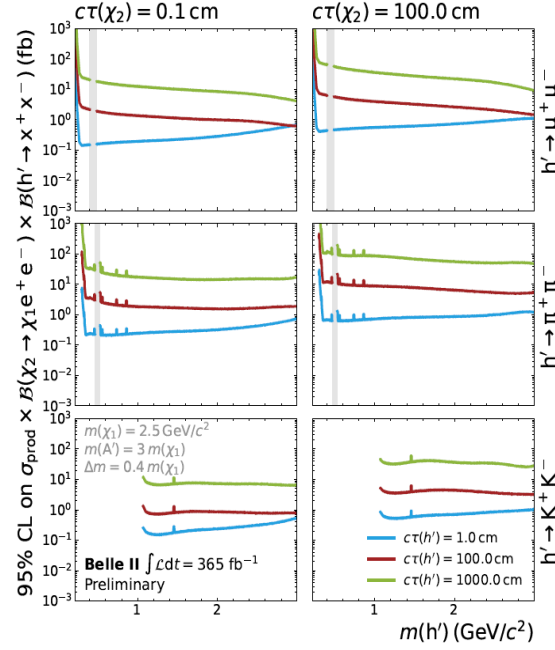


Figure 5: Observed 95% CL limits on the production cross section $\sigma_{prod}(e^+e^- \rightarrow h'\chi_1\chi_2) \times \mathcal{B}(\chi_2 \rightarrow \chi_1e^+e^-) \times \mathcal{B}(h' \rightarrow x^+x^-)$ as function of the dark Higgs mass $m_{h'}$ for various h' lifetimes with $c\tau(\chi_2)=0.1$ cm (left) and $c\tau(\chi_2) = 100$ cm (right). The mass region corresponding to the fully-vetoed K_S^0 is marked in gray.

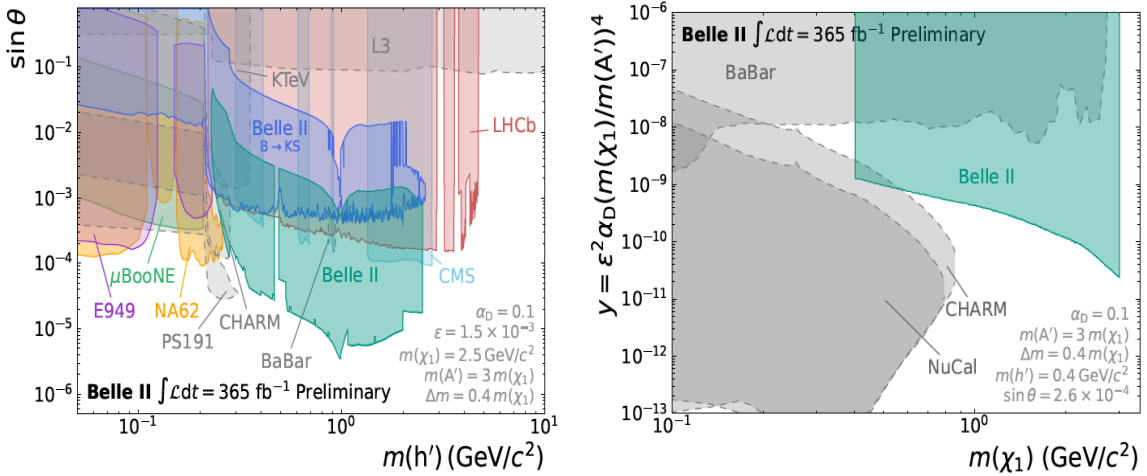


Figure 6: Exclusion regions at 95% CL in the $(\sin\theta - m_{h'})$ plane (left) and the $(y - m_{\chi_1})$ plane (right), where $y = \epsilon^2\alpha_D(m_{\chi_1}/m_{A'})^4$ is a dimensionless variable, from this work (teal) together with existing constraints from various experiments.

luminosity of 365 fb^{-1} . Due to the significantly low levels of background observed, we apply a cut and count technique to extract the signal. We do not find any significant excess compatible with signal events in 365 fb^{-1} of data, thus we set 95% CL upper limits on the cross section $\sigma(e^+e^- \rightarrow h'\chi_1\chi_2)$ and the branching fractions $\mathcal{B}(\chi_2 \rightarrow \chi_1e^+e^-) \times \mathcal{B}(h' \rightarrow x^+x^-)$ where $x = \mu, \pi, K$. Results can be seen in Figure 5. Similarly to the previous analysis, we translate these results to constrain the parameters of the model. Upper limits are set on the $(\sin\theta - m_{h'})$ parameter

space, that is defined by the sine of the mixing angle θ and the h' invariant mass, and $(y - m_{\chi_1})$ plane, where $y = \epsilon^2 \alpha_D (m_{\chi_1}/m_{A'})^4$ is a dimensionless variable. As shown in Figure 6 for a specific configuration of the model parameters, this analysis manages to probe two orders of magnitude more in $\sin\theta$ with respect to the existing limits set by other experiments.

4. Conclusions

The Belle II experiment provides excellent opportunities to explore the dark sector and study light dark matter and dark sector mediators. The sensitivity for such searches is complementary to that of higher-energy and beam-dump experiments. This paper presented the most recent results from Belle II dark sector searches, along with world-leading results and competitive limits on several models set using only a subset of the available data. Future advancements, including higher luminosity, improved analysis techniques, and new triggers for low-multiplicity events and displaced topologies, offer great potential for dark sector searches.

References

- [1] J. Beacham et al., *Physics beyond colliders at CERN: beyond the Standard Model working group report*, *Journal of Physics G: Nuclear and Particle Physics* **47** (2019) 010501.
- [2] S. Gori et al., *Dark Sectors 2016 Workshop: Community Report*, 2016. [arXiv:1608.08632](#).
- [3] K. Akai, K. Furukawa and H. Koiso, *SuperKEKB collider*, *Nuclear Instruments and Methods in Physics Research Section A: Accelerators, Spectrometers, Detectors and Associated Equipment* **907** (2018) 188.
- [4] I. Adachi et al., *Measurement of the integrated luminosity of data samples collected during 2019-2022 by the Belle II experiment*, *Chinese Physics C* **49** (2025) 013001.
- [5] X.G. He et al., *New- Z' phenomenology*, *Phys. Rev. D* **43** (1991) R22.
- [6] D. Forbes, C. Herwig, Y. Kahn, G. Krnjaic, C.M. Suarez, N. Tran et al., *New searches for muonphilic particles at proton beam dump spectrometers*, *Phys. Rev. D* **107** (2023) 116026.
- [7] BELLE II COLLABORATION collaboration, *Search for a $\mu^+\mu^-$ resonance in four-muon final states at Belle II*, *Phys. Rev. D* **109** (2024) 112015.
- [8] M. Pospelov et al., *Secluded WIMP dark matter*, *Physics Letters B* **662** (2008) 53.
- [9] BELLE II COLLABORATION collaboration, *Search for a long-lived spin-0 mediator in $b \rightarrow s$ transitions at the Belle II experiment*, *Phys. Rev. D* **108** (2023) L111104.
- [10] J. Jaeckel and A. Ringwald, *The Low-Energy Frontier of Particle Physics*, *Annual Review of Nuclear and Particle Science* **60** (2010) 405.
- [11] D. Smith and N. Weiner, *Inelastic dark matter*, *Phys. Rev. D* **64** (2001) 043502.
- [12] M. Duerr, T. Ferber and C.G.-C. et al., *Long-lived dark Higgs and inelastic dark matter at Belle II*, *Journal of High Energy Physics* **2021** (2021) 146.